Biochemical and Biophysical Research Communications 456 (2015) 573–579

Contents lists available at ScienceDirect

Biochemical and Biophysical Research Communications

journal homepage: www.elsevier.com/locate/ybbrc

Analysis of various types of single-polypeptide-chain (sc) heterodimeric $A_{2A}R/D_2R$ complexes and their allosteric receptor–receptor interactions

Toshio Kamiya [a,b,c,*,1], Kazuaki Yoshioka [a,2], Hiroyasu Nakata [a]

[a] Department of Molecular Cell Signaling, Tokyo Metropolitan Institute for Neuroscience, 2-6 Musashidai, Fuchu, Tokyo 183-8526, Japan
[b] Department of Neurology, Tokyo Metropolitan Institute for Neuroscience, 2-6 Musashidai, Fuchu, Tokyo 183-8526, Japan
[c] Cell Biology Laboratory, School of Pharmaceutical Sciences, Kinki University, 3-4-1 Kowakae, Higashi-Osaka, Osaka 577-8502, Japan

ARTICLE INFO

Article history:
Received 10 November 2014
Available online 2 December 2014

Keywords:
Oligomerization
Adenosine A_{2A} receptor
Dopamine D_2 receptor
Fluorescence resonance energy transfer
Fusion protein
Striatum

ABSTRACT

Adenosine A_{2A} receptor ($A_{2A}R$) heteromerizes with dopamine D_2 receptor (D_2R). However, these class A G protein-coupled receptor (GPCR) dimers are not fully formed, but depend on the equilibrium between monomer and dimer. In order to stimulate the heteromerization, we have previously shown a successful design for a fusion receptor, single-polypeptide-chain (sc) heterodimeric $A_{2A}R/D_2R$ complex. Here, using whole cell binding assay, six more different $scA_{2A}R/D_2R$ constructs were examined. Not only in $scA_{2A}R/D_2R$ 'liberated' with longer spacers between the two receptors, which confer the same configuration as the prototype, the $A_{2A}R$-*odr4*TM-$D_{2L}R$, but differ in size (Forms 1–3), but also in $scA_{2A}R/D_{2L}R$ (Form 6) fused with a transmembrane (TM) of another type II TM protein, instead of *odr4*TM, neither of their fixed stoichiometry (the apparent ratios of $A_{2A}R$ to D_2R binding sites) was 1, suggesting their compact folding. This suggests that type II TM, either *odr4* or another, facilitates the equilibrial process of the dimer formation between $A_{2A}R$ and $D_{2L}R$, resulting in the higher-order oligomer formation from monomer of $scA_{2A}R/D_{2L}R$ itself. Also, in the reverse type $scA_{2A}R/D_{2L}R$, i.e., the $D_{2L}R$-*odr4*TM-$A_{2A}R$, counter agonist-independent binding cooperativity (cooperative folding) was found to occur (Forms 4 and 5). In this way, the $scA_{2A}R/D_{2L}R$ system has unveiled the cellular phenomenon as a snapshot of the molecular behavior in $A_{2A}R/D_{2L}R$ dimer. Thus, these results indicate that the various designed types of functional $A_{2A}R/D_2R$ exist even in living cells and that this fusion expression system would be useful to analyze as a model of the interaction between class A GPCRs.

1. Introduction

Dopamine plays the critical role in the function in the striatum of the basal ganglia [1]. In the striatum, the stimulatory (G_s) heterotrimeric GTP-binding protein (G-protein)-coupled receptor (GPCR) for adenosine, subtype A_{2A} ($A_{2A}R$), [2] and the pertussis toxin-sensitive G_i (inhibitory)/G_o (G other)-coupled D_2 dopamine receptor (D_2R) [3] are highly coexpressed. By a model of receptor–receptor interaction, a functional antagonistic interaction between the $A_{2A}R$ and the D_2R to modulate dopaminergic activity has been explained based on various studies, where $A_{2A}R$ has been shown to bind directly to D_2R and form heteromeric complexes in brain tissues and cultured cells [4–7]. Also in living cells, we have previously shown the formation of homomeric $A_{2A}R$ complexes as well as heteromeric $A_{2A}R/D_2R$ complexes by bioluminescence resonance energy transfer (BRET) assay [8]. Importantly, unlike other class GPCRs, these class A GPCR dimers are not fully formed, but depend on the equilibrium between monomer and dimer [9]. Thus, to further characterize heteromeric $A_{2A}R/D_2R$ complexes, a fusion receptor was engineered consisting of a single-chain heterodimeric

Abbreviations: $A_{2A}R$, adenosine A_{2A} receptor; 3HA-$A_{2A}R$, $A_{2A}R$ tagged with a triple HA epitope; BRET, bioluminescence resonance energy transfer; BRET^2, improved BRET system offered by Packard Bioscience; C, carboxy-terminal; CD, cluster of differentiation; CGS21680, 2-[4-(2-carboxyethyl)phenethylamino]-5′-*N*-ethyl carboxamidoadenosine; $D_{2L}R$ and $D_{2S}R$, the long and short form of dopamine D_2 receptor, respectively; FRET, fluorescence resonance energy transfer; G_4S, an amino acid sequence consisting of a four-glycine-repeat followed by a serine residue; GABA, γ-aminobutyric acid; $GABA_B$, GABA type B receptor; GFP^2, modified green fluorescent protein; GPCR, G protein-coupled receptor; HA, hemagglutinin; IC, intracellular loops; MoAb, monoclonal antibody; M_r, molecular weight; N, amino-terminal; P2YR, GPCR for ATP; PD, Parkinson's disease; RGS, regulator of G-protein signaling; Rluc, *Renilla* luciferase; sc, single-chain; TM, transmembrane; XAC, xanthine amine congener; ZM241385, 4-(2-[7-amino-2-(2-furyl)[1,2,4]-triazolo[2,3-α][1,3,5]triazin-5-yl amino]ethyl)phenol.

* Corresponding author at: Division of Gene Regulation, Institute for Advanced Medical Research, Keio University School of Medicine, Keio University, 35 Shinano-machi, Shinjuku-ku, Tokyo 160-8582, Japan. Fax: +81 3 5363 3982.
E-mail addresses: kamiya@z2.keio.jp, kamiya@pharm.showa-u.ac.jp (T. Kamiya).
[1] Present address: Division of Gene Regulation, Institute for Advanced Medical Research, Keio University School of Medicine, Keio University, 35 Shinano-machi, Shinjuku-ku, Tokyo 160-8582, Japan.
[2] Present address: Department of Molecular Vascular Physiology, Kanazawa University Graduate School of Medical Science, 13-1 Takaramachi, Kanazawa, Ishikawa 920-8640, Japan.

http://dx.doi.org/10.1016/j.bbrc.2014.11.098
0006-291X/

$A_{2A}R/D_2R$ complex ($scA_{2A}R/D_2R$) by fusing the C-terminus of the $A_{2A}R$ via transmembrane domain (TM) of a type II TM protein with the N-terminus of D_2R in tandem, and it succeeded to be expressed on the cell surface as a full-length protein with specific binding to the respective ligands and functional coupling to G-proteins comparable to wild-type receptors [10].

Lipid vesicles are fusogenic, which are formed by the ability of lipids to spontaneously assemble into membrane bilayer structures (liposomes) [11]. Irrespective of the lipid vesicles, some receptors in the membrane preparations from cells or tissues do not work well for ligand binding assays, although powerful methods. In previous study, obtained cell membranes needed to be used immediately because D_2R binding activity alone of $scA_{2A}R/D_2R$ was lost soon [10]. Thus, by whole cell binding assay to circumvent such technical difficulty, we showed that in the transfected cells, $scA_{2A}R/D_2R$ forms a functional $A_{2A}R/D_2R$ complex. This suggests that $scA_{2A}R/D_2R$ is physiologically relevant *in vitro*. In addition, we discuss a relationship between the configuration of each component and subsequent binding cooperativity [12] in the context of $scA_{2A}R/D_2R$.

2. Materials and methods

2.1. Construction of vectors for $scA_{2A}R/D_{2L}R$

HA-tagged $A_{2A}R$, triple HA (3HA)-tagged $A_{2A}R$, Myc-tagged $D_{2L}R$, and single-chain $A_{2A}R/D_{2L}R$ [HA-tagged $A_{2A}R$-*odr4*TM-$D_{2L}R$, HA-$A_{2A}R$-$D_{2L}R$(ΔTM1), and Myc-$D_{2L}R$-$A_{2A}R$(ΔTM1)] and BRET constructs for $A_{2A}R$ and $D_{2L}R$ were described previously [8,10]. In order to reduce potential rigidity of HA-$A_{2A}R$-*odr4*TM-$D_{2L}R$ between the C-terminus of $A_{2A}R$ and the *odr4*TM, and/or between the *odr4*TM and the N-terminus of $D_{2L}R$, a spacer sequence GGGGSGGGGS was introduced in various locations. This created several new forms of the single-chain construct: HA-$A_{2A}R$-*odr4*TM-s-$D_{2L}R$ (Fig. 1A, Forms 1 and 2) and HA-$A_{2A}R$-s-*odr4*TM-s-$D_{2L}R$ (Form 3). Reverse constructs, Myc-tagged $D_{2L}R$-*odr4*TM-$A_{2A}R$ (Form 4) and Myc-$D_{2L}R$-s-*odr4*TM-s-$A_{2A}R$, were also generated, which included the spacer sequence (Form 5), by using Myc-$D_{2L}R$-$A_{2A}R$(ΔTM1) [8]. The *odr4*TM of HA-$A_{2A}R$-*odr4*TM-$D_{2L}R$ was replaced with the TM domain of the human low affinity receptor for IgE designated CD23, creating HA-$A_{2A}R$-*cd23*TM-$D_{2L}R$ (Form 6). 3HA-tagged $A_{2A}R$-*odr4*TM-$D_{2L}R$ was also generated. The following primers for PCR were used (the restriction enzyme site is underlined and the initiating Met codon and stop codon are shown in bold): 5′-C-G GGATCC GTTAAC ACTCAGATTGTTCTTCTTGGACTTGTTACTGCTGC-T CTTTGGGCTGGAC (F-CD23-TM, 63mer, HPLC-purified); 5′-CGGG-A TCC AT AGCGCT CCAGTGCCAAAGAAGAAGAAGAGTAAGAAGTCC-A GCCCAAAGAGCAGCAG (R-CD23-TM, 66mer, HPLC-purified); 5′-G GATATC GGAGGAGGAGGATCTGGAGGAGGAGGATCTAGCGCTG-AT ATCC (F-G4S2, 50 mer, HPLC-purified); 5′-GGATATC AGCGCTAG-A TCCTCCTCCTCCAGATCCTCCTCCTCCGATATCC (R-G4S2, 50 mer, HPLC-purified). All PCR-amplified sequences were confirmed by sequencing analysis.

2.2. Cell culture, transfection, and radioligand binding assay

Transient expression studies with human embryonic kidney (HEK) 293T cells were performed as previously described [10]. Maintenance of SH-SY5Y cells is described in detail elsewhere (H.N.). These cultured cells were not validated for evidence of authenticity, and tests in being free of mycoplasma contamination to them were also not done, although no ordinary microbial/bacterial contamination was observed at any passage (International Cell Line Authentication Committee, http://iclac.org/).

Fig. 1. Constructs of various types of $scA_{2A}R/D_2R$. (A) In order to reduce potential rigidity of HA-$A_{2A}R$-*odr4*TM-$D_{2L}R$ between C-terminus of $A_{2A}R$ and *odr4*TM, and/or between *odr4*TM and N-terminus of $D_{2L}R$, we introduced a spacer sequence GGGGSGGGGS, resulting in HA-$A_{2A}R$-*odr4*TM-s-$D_{2L}R$ (Forms 1 and 2) and HA-$A_{2A}R$-s-*odr4*TM-s-$D_{2L}R$ (Form 3). We also generated reverse constructs Myc-tagged $D_{2L}R$-*odr4*TM-$A_{2A}R$ (Form 4) and Myc-$D_{2L}R$-s-*odr4*TM-s-$A_{2A}R$ carrying the spacer sequence (Form 5). We replaced *odr4*TM of HA-$A_{2A}R$-*odr4*TM-$D_{2L}R$ with TM of the human low affinity receptor for IgE designated CD23, resulting in HA-$A_{2A}R$-*cd23*TM-$D_{2L}R$ (Form 6). Note $(G_4S)_3$: 3.5 nm. (B) SDS–PAGE (10% gel)/immunoblot of constructs. Immunoblot analysis of crude membranes from the transfected 293T cells of $scA_{2A}R/D_{2L}R$, i.e., prototype $A_{2A}R$-*odr4*TM-$D_{2L}R$ (3HA-tagged: lane 3), Forms 1–3 and 6 (lanes 4–7, respectively), with anti-HA antibody showed the bands corresponding to the respective receptors, but no additional band with much lower molecular masses, corresponding to the anticipated monomeric receptors, indicating the full-length protein $scA_{2A}R/D_{2L}R$. GFP (lane 1) and coexpressed 3HA-$A_{2A}R$/Myc-$D_{2L}R$ (lane 2) in 293T cells are also shown. In (B), 21 μg membrane protein each/lane, except for lane 1 (11 μg), were applied.

2.3. Immunofluorescence

Immunofluorescence studies were performed as previously described [10]. The transfected cells were washed once with

serum-free D-MEM, and then incubated for 3 h at 37 °C in the absence or presence of 1 μM CGS21680, 10 μM quinpirole, or 10 μM ADP-β-S. Cells were then fixed. A semi-quantitative analysis of images on the distribution of coexisting receptors obtained, by evaluating the intensity of the color and calculating "the Gini's index (a measure of unevenness, which evaluates the proportion of coaggregates in the sampled area)," [7] was not done.

2.4. Whole cell binding assay

Whole cell binding assays (D_2R saturation binding assays) were performed essentially according to Guo et al. [13]. To put it briefly, the transfected cells were treated with the agonists as described above, and processed except for incubation being carried out with [^{3}H]spiperone (851 GBq mmol^{-1}; Amersham Pharmacia Biotech), using 10–20 μg of intact whole cells per tube for 1 h at 25 °C. Non-specific binding was defined as binding in the presence of 100 nM haloperidol. In $A_{2A}R$ saturation experiments at 4 °C with [^{3}H]ZM241385 (23.47 Ci/mmol; Tocris, Bristol), non-specific binding was defined as binding in the presence of 10 μM xanthine amine congener. All the binding data were analyzed with Prism 3.0 (GraphPad Software). No apparent endogenous $A_{2A}R$ and D_2R were observed in the host HEK 293T cells used in this study (The expression level of receptors is discussed in Supplemental Information), by either the respective receptor-specific radioligand binding assay (Fig. S3C) or immunoblot analysis [10: Fig. 1B].

2.5. Immunoblot analysis

Cell membranes were subjected to SDS–PAGE and transferred to a nitrocellulose membrane as previously described [10]. The immunoreactive bands on blots were probed with rabbit anti-$A_{2A}R$ and rabbit anti-D_2R antibodies (Alpha Diagnostic) or rat anti-HA 3F10 MoAb (Roche Diagnostics). In Fig. 1B, the crude membranes [8] that were dissolved in urea (~8.5 M)-containing sample buffer [14], instead of Laemmli's sample buffer, were also used to subject to SDS–PAGE. In Fig. 2A, membranes from stable Myc-$D_{2L}R$-expressing 293 cells transiently transfected with 3HA-$A_{2A}R$ were solubilized [8] in 50 mM Tris–HCl (pH 7.4) + 0.1 M NaCl + 1% digitonin + ≪0.2% cholesteryl hemisuccinate. The resultant lysate was incubated with anti-HA MoAb-beads (Roche Diagnostics) and eluted with HA peptide (Rounds 1 and 2). Insoluble fraction (ppt) was also analyzed after further solubilization.

3. Results and discussion

3.1. Various types of $scA_{2A}R/D_2R$

3.1.1. $scA_{2A}R/D_{2L}R$ Forms 1–3, with the same configuration as the prototype, the $A_{2A}R$-*odr4*TM-$D_{2L}R$

In $scA_{2A}R/D_{2L}R$, the *odr4*TM mediates connection between the N-terminal receptor half ($A_{2A}R$) and the C-terminal receptor half ($D_{2L}R$, the long form of D_2R) of the fused receptor. To analyze the effect of the *odr4*TM on the binding activity of the fused receptor, we generated three other forms: 1–3, respectively, which consisted of a spacer (linker sequence) of 14 (Form 1) or 26 amino acids (Form 2), including glycine-glycine-glycine-glycine-serine (G_4S), between the *odr4*TM and the N-terminus of $D_{2L}R$, and an additional spacer of 26 amino acids (Form 3), including G_4S, between the C-terminus of $A_{2A}R$ and the *odr4*TM (Fig. 1A). These constructs were transiently transfected into HEK293T cells, and radioligand binding assay using the intact whole cells was carried out as described in Section 2 (Table 1). In previous study, obtained cell membranes needed to be used immediately because D_2R binding activity alone of $scA_{2A}R/D_2R$ was lost soon [10]. Whole cell binding assay was found to be able to avoid this technical difficulty, by taking benefit from D_2R saturation binding assay [(at 25 °C using cell membranes) of Armstrong and Strange] [15] that allows to distinguish between D_2R monomer and dimer formation. All of these constructs showed no significant changes in ligand binding characteristics (K_d, B_{max}, and the apparent ratio of the $A_{2A}R$ to D_2R binding sites in the $scA_{2A}R/D_{2L}R$, $B_{max}A_{2A}R/B_{max}D_2R$) compared to the prototype $scA_{2A}R/D_{2L}R$. This suggests that the incorporation of longer amino acid sequences around *odr4*TM did not affect the expression (and/or stability of ligand-binding pockets) of $scA_{2A}R/D_{2L}R$, given $(G_4S)_3$: 3.5 nm [16]. Again, although highly 'liberated' $scA_{2A}R/D_{2L}R$ (with longer spacer between the two receptors: Forms 1–3) should have the $B_{max}A_{2A}R/B_{max}D_2R$ of 1, neither was found to do. These suggested $scA_{2A}R/D_{2L}R$ as heteromeric $A_{2A}R/D_2R$, such that it keeps on the steric hindrance of D_2R binding pockets, partly includes the less stable folding of $scA_{2A}R/D_{2L}R$ and/or the higher order oligomerization of $scA_{2A}R/D_{2L}R$, with a tendency to aggregate in sample preparation for SDS–PAGE and immunoblot analysis (Section 3.1.4).

3.1.2. $scA_{2A}R/D_{2L}R$ Forms 4 and 5, the $D_{2L}R$-*odr4*TM-$A_{2A}R$, with the different configuration from the prototype

Next, in order to elucidate the reasons for $B_{max}A_{2A}R/B_{max}D_2R$ of 4 in the $scA_{2A}R/D_{2L}R$, regardless of these two GPCRs expressed in a single-polypeptide-chain with a fixed stoichiometric ratio, i.e., whether it is due to configuration (position) of the two receptors, we generated the reverse type $scA_{2A}R/D_{2L}R$: Forms 4 and 5 which contained $D_{2L}R$ and $A_{2A}R$ at the respective N- and C-terminus of the *odr4*TM, including shorter sequence of 8 amino acids (Form 4) and longer sequence of 18 and 16 amino acids (Form 5) (Fig. 1A). These constructs showed active $A_{2A}R$-specific binding activity similar to (Form 4) or lower (Form 5, as a tendency although not significant), but no (Form 4) or indistinguishable but faint (Form 5) D_2R-specific binding activity compared with, the respective wild-type receptors and the prototype $scA_{2A}R/D_{2L}R$. It suggested that the length of amino acid sequence connecting $D_{2L}R$ to $A_{2A}R$ via *odr4*TM was not sufficient to guarantee the structure and the activity of the $D_{2L}R$-*odr4*TM-$A_{2A}R$, which in turn is less stable than $A_{2A}R$-*odr4*TM-$D_{2L}R$.

3.1.3. $scA_{2A}R/D_{2L}R$ with another TM, Form 6

Moreover, in order to determine whether an insertion of some other TM sequence instead of the *odr4*TM sequence works similarly, or whether it has to be *odr4*TM to work, we also designed $scA_{2A}R/D_{2L}R$ with another TM: Form 6 which included TM of the human low affinity receptor for IgE designated CD23 as a type II TM protein (Fig. 1A). This construct showed the similar ligand binding characteristics (K_d, B_{max}, and $B_{max}A_{2A}R/B_{max}D_2R$) to the prototype $scA_{2A}R/D_{2L}R$, suggesting that the sequence of TM of type II TM proteins did not affect the expression (and/or stability of ligand-binding pockets) (stability) of $scA_{2A}R/D_{2L}R$.

3.1.4. Comparisons between the $scA_{2A}R/D_{2L}R$ constructs

No [K_d = 0.3 ± 0.2 nM, $A_{2A}R$–$D_{2L}R$(ΔTM1); 0.4 ± 0.08, Forms 4 vs. 0.3 ± 0.03 nM, wild-type] and strong negative binding cooperativity (K_d = 2.4 ± 2 nM, Forms 5 vs. 0.3 ± 0.03 nM, wild-type; as a tendency although not significant) occurred in the context of $scA_{2A}R/D_{2L}R$, i.e., $A_{2A}R$–$D_{2L}R$(ΔTM1) (Table 1; data not shown); [10] or the reverse type $D_{2L}R$-*odr4*TM-$A_{2A}R$ with shorter and longer sequence between the two receptors, Forms 4, and 5, respectively. On the other hand, the full-length proteins $scA_{2A}R/D_{2L}R$s, i.e., prototype $A_{2A}R$-*odr4*TM-$D_{2L}R$, and Forms 1–3 and 6, have similar binding characteristic to wild-type receptors (without reduction of the affinity of $A_{2A}R$; no allostery within a 100% $A_{2A}R/D_{2L}R$ heteromeric complex). In spite of a tendency to aggregate in sample preparation

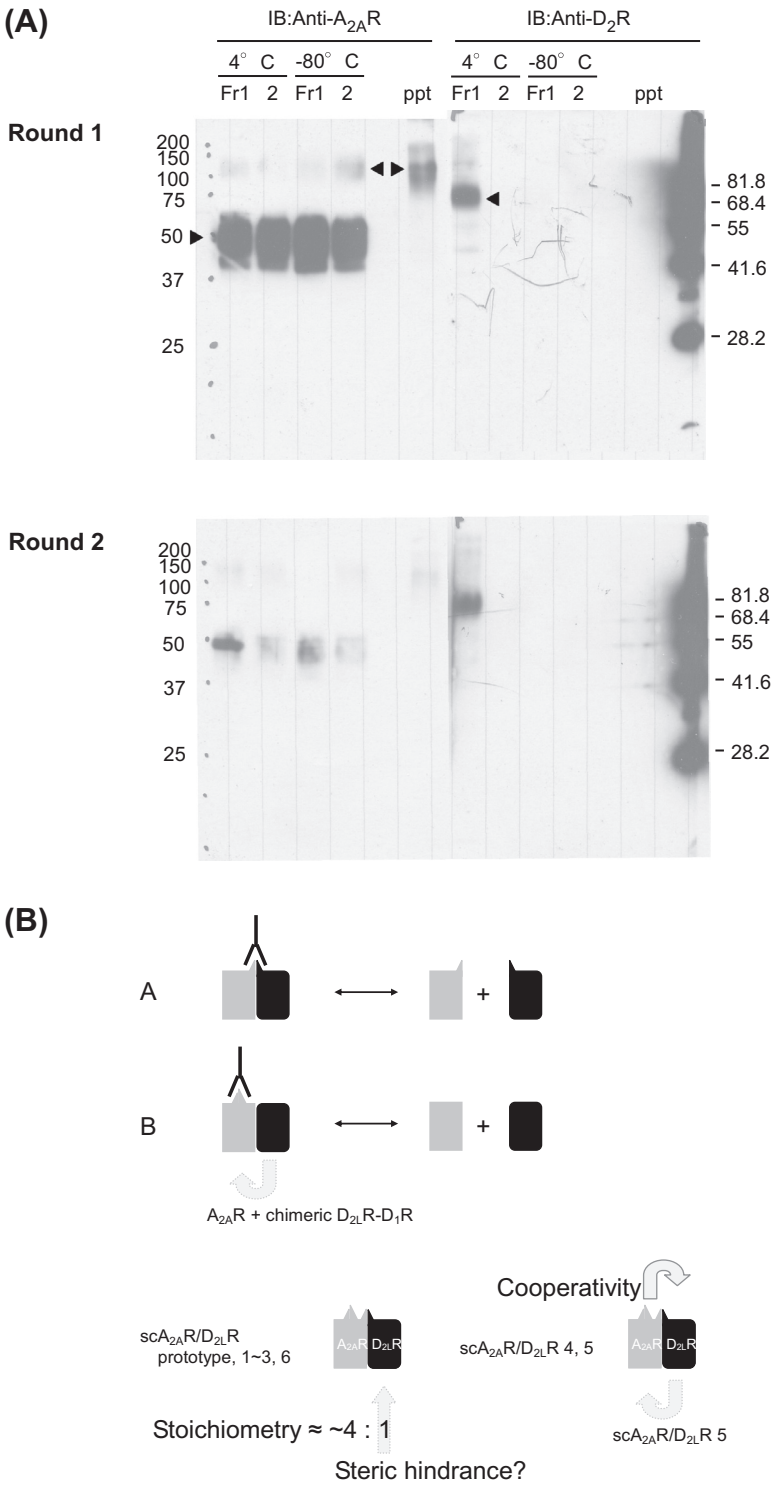

Fig. 2. Partial purification of $A_{2A}R/D_{2L}R$. This allows it to elucidate molecular entity of the antagonism between $D_{2L}R$ and $A_{2A}R$. (A) Immunopurified heteromeric $A_{2A}R/D_{2L}R$ complex can be stored at 4 °C but not at −80 °C. Cell membranes of coexpressed $A_{2A}R/D_{2L}R$ were solubilized and partially purified with anti-HA MoAb column. The elution (Rounds 1 and 2), and insoluble fraction (ppt) that had been thus followed by further solubilization, were analyzed with immunoblot: a band of $D_{2L}R$ but not $A_{2A}R$ disappeared upon freezing. Also, note the $A_{2A}R$ distribution (more dimer in ppt). Arrowheads indicate the monomer (lower) and the dimer (upper) of the wild-type receptors {[8]-B}. Note that stable Myc-$D_{2L}R$ expressed in HEK 293 cells is a heavily N-glycosylated protein with a major band of ~70 kDa ([8]-B, lane 8; vs. 53 kDa theoretical M_r), different from that of transient one. The partially purified $A_{2A}R/D_{2L}R$ (yield ~60% of the start) had, although not full, a [^{3}H]ZM241385-binding activity (data not shown); their antagonism remains unresolved because competition experiments with dopamine vs. [^{3}H]raclopride (displacement assay) were not done. (B) Appearance of epitopes in heteromeric $A_{2A}R/D_{2L}R$ alone (the upper and lower), but not in monomeric (and/or homodimeric) $A_{2A}R$ or $D_{2L}R$, can occur. In order to obtain an MoAb specific for heteromeric $A_{2A}R/D_{2L}R$, because of the above reason, partially purified $A_{2A}R/D_{2L}R$ was not used for an immunogen. Thus, mice were immunized with membranes of the coexressed receptors. Also, prototype $scA_{2A}R/D_{2L}R$ was not used as an immunogen at that time because whether $scA_{2A}R/D_{2L}R$ can simulate wild-type $A_{2A}R/D_{2L}R$ remains unresolved as described in this paper. The existence of several conformational states of $scA_{2A}R/D_{2L}R$ and its relation to the striatal antagonism are discussed in Supplemental Information.

Table 1
Radioligand binding to receptors expressed on the cell surface.[a]

Transfected receptors (treatment)	[^{3}H]ZM241385		[^{3}H]spiperone	
	K_d (nM)	B_{max} (pmol/mg)	K_d (nM)	B_{max} (pmol/mg)
3HA-A_{2A}R + Myc-D_{2L}R	0.3 ± 0.03	3.7 ± 0.9	0.1 ± 0.03[b]	0.9 ± 0.3
HA-A_{2A}R-D_{2L}R(ΔTM1)	0.3 ± 0.2	0.3 ± 0.1	–[c]	–
Myc-D_{2L}R-A_{2A}R(ΔTM1)	–	–	0.3 ± 0.05	0.1 ± 0.0
HA-A_{2A}R-*odr4*TM-D_{2L}R	0.3 ± 0.09	1.3 ± 0.1[d]	0.2 ± 0.05[b]	0.5 ± 0.1[d]
3HA-A_{2A}R-*odr4*TM-D_{2L}R	0.3 ± 0.1	1.4 ± 0.4[e]	0.1 ± 0.01[b]	0.4 ± 0.1[e]
scA_{2A}R/D_{2L}R 1	0.2 ± 0.04	1.7 ± 0.5	0.2 ± 0.04	0.8 ± 0.2
scA_{2A}R/D_{2L}R 2	0.2 ± 0.02	0.9 ± 0.1	0.2 ± 0.02	0.5 ± 0.1
scA_{2A}R/D_{2L}R 3	0.2 ± 0.03	1.5 ± 0.5	0.2 ± 0.01	0.7 ± 0.3
scA_{2A}R/D_{2L}R 4	0.4 ± 0.08	0.8 ± 0.4	–	–
scA_{2A}R/D_{2L}R 5	2.4 ± 2	1.6 ± 1	0.2 ± 0.2	0.0 ± 0.0
scA_{2A}R/D_{2L}R 6	0.1 ± 0.00	0.4 ± 0.0	0.08 ± 0.01	0.2 ± 0.1
HA-A_{2A}R-A_1R + Myc-D_{2L}R	–	–	0.1 ± 0.03	0.7 ± 0.3
3HA-A_{2A}R + Myc-D_{2L}R-D_1R	0.6 ± 0.2	10 ± 1	–	–

Transfected receptors	B_{max}/B_{max}[f] (arbitrary)
3HA-A_{2A}R + Myc-D_{2L}R	6 ± 3
HA-A_{2A}R-D_{2L}R(ΔTM1)	–[g]
Myc-D_{2L}R-A_{2A}R(ΔTM1)	–
HA-A_{2A}R-*odr4*TM-D_{2L}R	3 ± 0.5
3HA-A_{2A}R-*odr4*TM-D_{2L}R	4 ± 0.8
scA_{2A}R/D_{2L}R 1	2 ± 0.2
scA_{2A}R/D_{2L}R 2	2 ± 0.4
scA_{2A}R/D_{2L}R 3	3 ± 1
scA_{2A}R/D_{2L}R 4	–
scA_{2A}R/D_{2L}R 5	18 ± 8
scA_{2A}R/D_{2L}R 6	4 ± 2
HA-A_{2A}R-A_1R + Myc-D_{2L}R	–
3HA-A_{2A}R + Myc-D_{2L}R-D_1R	–

[a] A_{2A}R and D_2R saturation binding assays were carried out with radioligands [^{3}H]ZM241385 and [^{3}H]spiperone, respectively, using intact whole HEK293T cells. Data are expressed as mean ± SEM of 2–3 independent experiments: [^{3}H]spiperone binding of the transfected receptors, Myc-D_{2L}R-A_{2A}R(ΔTM1) and scA_{2A}R/D_{2L}R 5, and [^{3}H]ZM241385- or [^{3}H]spiperone binding of the transfected receptors (HA-A_{2A}R-A_1R + Myc-D_{2L}R; 3HA-A_{2A}R + Myc-D_{2L}R-D_1R) were carried out in two binding experiments of the different cell preparations, obtained in two independent transfection experiments; (others were done three times: three binding experiments from three independent transfection experiments).

[b] The difference between the groups is not statistically significant ($P < 0.05$, Student's t-test). Student's t-test was done every between two groups, but not between more than two.

[c] No specific binding for ligands observed.

[d,e] The difference between the groups is statistically significant (d: $P < 0.01$; e: $P < 0.05$, Student's t-test).

[f] The apparent ratio of the A_{2A}R to D_2R binding sites (B_{max} of [^{3}H]ZM241385 binding/B_{max} of [^{3}H]spiperone binding, arbitrary unit) was determined.

[g] The apparent ratio (B_{max}/B_{max}) was not determined because of no specific binding for ligands observed.

for SDS–PAGE and immunoblot analysis, molecular populations of scA_{2A}R/D_{2L}R species were determined. Immunoblot analysis of crude membranes [8] from the transfected cells (Forms 1–3 and 6) with anti-A_{2A}R and anti-D_2R antibodies indicated the bands corresponding to the respective receptor oligomers, {probably including 240 kDa in M_r, much higher than approximately 82 kDa, vs. the theoretical M_r of the prototype scA_{2A}R/D_{2L}R, A_{2A}R-*odr4*TM-D_{2L}R (101 kDa) [10]}, but no additional band with much lower molecular masses, corresponding to the anticipated monomeric receptors (data not shown); whereas that of the reverse type scA_{2A}R/D_{2L}R, either Forms 4 or 5, did additional smaller ones. In other experiments of immunoblot analysis with anti-HA antibody, Forms 1–3 and 6 with the full-length protein were confirmed (Fig. 1B): however, Form 2 (lane 5) showed the thickest band among scA_{2A}R/D_{2L}Rs, indicating the greatest expression in crude membrane, irrespective of radioligand binding (Table 1). Why binding of specific ligands to Forms 1–3, except for the minimum in Form 6, did not necessarily represent the receptor expression measured by the HA antibody, i.e., the difference of the degree of HA-immunoreactivities between the scA_{2A}R/D_{2L}Rs (Supplemental Information), was not addressed in detail because of the difficulty in dealing with these samples. Overall, these results suggest that highly specific binding to the respective ligands of various types of scA_{2A}R/D_{2L}R (Forms 1–3 and 6), unlike Forms 4 and 5, is shown by full-length single polypeptide chain, and not by degraded monomeric A_{2A}R and D_{2L}R, in membrane preparation. This point is discussed more in detail in relation to CFP- and YFP-tagged receptors, originally for FRET analysis (as described in Supplemental Results: Figs. S1/S2). Together with this point, expression level of receptors is also discussed in Supplemental Information. Ligand binding characteristics determined by using intact whole cells indicated that transfectants exhibited a membrane-associated form of the receptors, the ligand-binding site of which clearly faced the extracellular domain.

Furthermore, among these constructs Forms 1–3 and 6 had the same stability to the prototype scA_{2A}R/D_{2L}R by immunoblot analysis, while Forms 1–3 and 6 showed the similar ligand binding characteristics to the prototype. Prior experiments indicated that partially purified A_{2A}R/D_{2L}R (A_{2A}R was also contained) obtained by immunopurification with anti-HA column following solubilization of membranes from (transient) 3HA-A_{2A}R/(stable) Myc-D_{2L}R-expressing 293 cells [8,17] was unexpectedly unable to be stored at −80 °C, while no D_{2L}R but A_{2A}R-bands could be detected upon freezing (Fig. 2A). In this context, membranes of scA_{2A}R/D_{2L}R were also unstable. In our previous reports [8,10,17], extensively washed membranes from the transfected cells were used on immunoblot analysis as well as on radioligand binding assay. Also, Forms 1–3 and 6 showed the $B_{max}A_{2A}$R/$B_{max}D_2$R of 2–4: Type II TM, either *odr4* or CD23, did not interact itself with the test ligands. Taken together, these results suggested that it is important how to connect via TM of a type II TM protein by introducing the linker sequences with the length enough to sustain configuration, rather

Table 2
Radioligand binding to receptors expressed on the cell surface.[a]

Transfected receptors (Treatment)	[^{3}H]spiperone	
	K_d (nM)	B_{max} (pmol/mg)
3HA-A_{2A}R + Myc-D_{2L}R	0.06 ± 0.00	0.5 ± 0.1
None	0.08 ± 0.02[b]	0.5 ± 0.1[c]
Quinpirole	0.08 ± 0.02[b]	0.5 ± 0.2[c]
HA-A_{2A}R-*odr4*TM-D_{2L}R	0.05 ± 0.05	0.3 ± 0.2
None	0.06 ± 0.01[d]	0.3 ± 0.2[e]
Quinpirole	0.09 ± 0.06[d]	0.3 ± 0.2[e]

[a] After treatment with the D_2R agonist quinpirole (10 μM for 3 h), D_2R saturation binding assays were carried out with radioligands [^{3}H]spiperone, using intact whole SH-SY5Y cells. Data are expressed as mean ± SEM of 2 independent experiments.
[b,c,d,e] The difference between the groups is not statistically significant ($P < 0.05$, Student's *t*-test).

than the sequence itself of TM of type II TM proteins between the two receptors, and that the prototype scA_{2A}R/D_{2L}R was the best fusion to analyze further as a model of heteromeric A_{2A}R/D_{2L}R among these constructs (Fig. 2B). Because our major concern is the allostery within the scA_{2A}R/D_{2L}R (Their existence of several conformational states is discussed in Supplemental Information), scA_{2A}R/D_{2L}R constructs consisting of the respective chimeric receptor halves (Supplemental Information) were not generated. Also, FRET constructs by the incorporation at an appropriate place in the context of this reorganized scA_{2A}R/D_{2L}R were not generated. However, in the present study without single molecule analysis, two other points unresolved in our previous report [10] have been clarified (Supplemental Information, Fig. S5).

3.1.5. Expression of scA_{2A}R/D_2R in SH-SY5Y cells

In order to confirm the existence of functional scA_{2A}R/D_{2L}R complexes, that is, even though degraded ones or as a dimer or oligomer of scA_{2A}R/D_{2L}R, like a wild-type heterodimer of A_{2A}R and D_{2L}R, HA-A_{2A}R-*odr4*TM-D_{2L}R was transfected into the human neuroblastoma cell line SH-SY5Y cells, and radioligand binding assays using intact whole cells were carried out to address whether in HA-A_{2A}R-*odr4*TM-D_{2L}R-expressed SH-SY5Y cells treatment with the D_2R agonist quinpirole induced coaggregation of the receptors. Table 2 shows that membrane-associated and extracellularly faced form of the D_2R did not significantly change after treatment with the D_2R agonist quinpirole in both HA-A_{2A}R-*odr4*TM-D_{2L}R-expressed and wild-type 3HA-A_{2A}R/Myc-D_{2L}R-coexpressed SH-SY5Y cells, suggesting no internalization of the D_2R, consistent with results obtained by immunofluorescence analysis as described in Supplemental Information. SEM values of [^{3}H]spiperone-binding activities of HA-A_{2A}R-*odr4*TM-D_{2L}R were larger than the values of samples in Table 1 and wild-type in Table 2. Whether this was due to this assay itself, which in turn to obtain more reduced SEM, its further modifications and appropriate alternatives should be done, or stability of HA-A_{2A}R-*odr4*TM-D_{2L}R was not addressed. Here, we could not exclude the possibility of rapid internalization followed by recycling to the cell surface (discussed in Supplemental Information) during an incubation for 1 h at 25 °C by whole cell binding assay.

In summary, the present study clarifies a relationship between counter agonist-independent binding cooperativity and configuration of each component in various types of constructs (discussed in Supplemental Information), and indicates that various designed types of functional A_{2A}R/D_2R exist even in living cells and that this fusion expression system would be useful to analyze as a model.

Conflict of interest

The authors declare no competing financial interests.

Acknowledgments

We thank Dr. A. Miyawaki (RIKEN, Wako); Drs. K. Fuxe and M. Torvinen (Karolinska Institutet, Stockholm); Drs. O. Saitoh (Nagahama Institute of Bio-Science and Technology, Nagahama), T. Masuko (Kinki University, Higashi-Osaka) and T. Hirokawa (Computational Biology Research Center, National Institute of Advanced Industrial Science and Technology, Tokyo) for their respective contributions, Dr. H. Okado (Tokyo Metropolitan Institute of Medical Science, Tokyo); Drs. K. Fuxe and D.O. Borroto-Escuela; Mr. M. Woolfenden; and Dr. H. Saya (Keio University, Tokyo). This work was supported in part by grants for Scientific Research from the Ministry of Education, Culture, Sports, Science and Technology (MEXT) (#14657595, 13670109: to T.K., O.S., and H.N.). This work was also supported in part by grants of intramural budget (TMIN to T.K., O.S., and H.N.). T.M. was also supported by the "Academic Frontier" Project for Private Universities: matching fund subsidy from MEXT, 2005–2007. H.N. was also supported by a CREST program of the Japan Science and Technology Agency. A full description is in Supplemental Information, including author contributions (All of the experiments were finished by the end of March 2007 when H.N. retired under the age limit, and even additional supporting experiments of this study were completely finished by the end of March 2008; All authors commented on the manuscript, except for H.N. who is at present under a departure from research activity, and for K.Y. who is at present under a departure from this research activity.).

Appendix A. Supplementary data

Supplementary data associated with this article can be found, in the online version, at http://dx.doi.org/10.1016/j.bbrc.2014.11.098.

References

[1] A.C. Kreitzer, R.C. Malenka, Striatal plasticity and basal ganglia circuit function, Neuron 60 (2008) 543–554.
[2] V. Ralevic, G. Burnstock, Receptors for purines and pyrimidines, Pharmacol. Rev. 50 (1998) 413–492.
[3] C. Missale, S.R. Nash, S.W. Robinson, M. Jaber, M.G. Caron, Dopamine receptors: from structure to function, Physiol. Rev. 78 (1998) 189–225.
[4] L.F. Agnati, S. Ferré, C. Lluis, R. Franco, K. Fuxe, Molecular mechanisms and therapeutical implications of intramembrane receptor/receptor interactions among heptahelical receptors with examples from the striatopallidal GABA neurons, Pharmacol. Rev. 55 (2003) 509–550.
[5] M. Canals, D. Marcellino, F. Fanelli, F. Ciruela, P. de Benedetti, S.R. Goldberg, K. Neve, K. Fuxe, L.F. Agnati, A.S. Woods, S. Ferré, C. Lluis, M. Bouvier, R. Franco, Adenosine A_{2A}-dopamine D_2 receptor–receptor heteromerization: qualitative and quantitative assessment by fluorescence and bioluminescence energy transfer, J. Biol. Chem. 278 (2003) 46741–46749.
[6] M. Canals, J. Burgueño, D. Marcellino, N. Cabello, E.I. Canela, J. Mallol, L. Agnati, S. Ferré, M. Bouvier, K. Fuxe, F. Ciruela, C. Lluis, R. Franco, Homodimerization of adenosine A_{2A} receptors: qualitative and quantitative assessment by fluorescence and bioluminescence energy transfer, J. Neurochem. 88 (2004) 726–734.
[7] J. Hillion, M. Canals, M. Torvinen, V. Casadó, R. Scott, A. Terasmaa, A. Hansson, S. Watson, M.E. Olah, J. Mallol, E.I. Canela, M. Zoli, L.F. Agnati, C.F. Ibáñez, C. Lluis, R. Franco, S. Ferré, K. Fuxe, Coaggregation, cointernalization, and codesensitization of adenosine A_{2A} receptors and dopamine D_2 receptors, J. Biol. Chem. 277 (2002) 18091–18097.
[8] T. Kamiya, O. Saitoh, K. Yoshioka, H. Nakata, Oligomerization of adenosine A_{2A} and dopamine D_2 receptors in living cells, Biochem. Biophys. Res. Commun. 306 (2003) 544–549.
[9] S. Ferré, V. Casadó, L.A. Devi, M. Filizola, R. Jockers, M.J. Lohse, G. Milligan, J.-P. Pin, X. Guitart, G protein-coupled receptor oligomerization revisited: functional and pharmacological perspectives, Pharmacol. Rev. 66 (2014) 413–434.
[10] T. Kamiya, O. Saitoh, H. Nakata, Functional expression of single-chain heterodimeric G-protein-coupled receptor for adenosine and dopamine, Cell Struct. Funct. 29 (2005) 139–145.
[11] L.V. Chernomordik, M.M. Kozlov, Mechanics of membrane fusion, Nat. Struct. Mol. Biol. 15 (2008) 675–683.
[12] D. Wootten, A. Christopoulos, P.M. Sexton, Emerging paradigms in GPCR allostery: implications for drug discovery, Nat. Rev. Drug Discov. 12 (2013) 630–644.

[13] W. Guo, L. Shi, J.A. Javitch, The fourth transmembrane segment forms the interface of the dopamine D2 receptor homodimer, J. Biol. Chem. 278 (2003) 4385–4388.
[14] E. Harlow, D. Lane, Using Antibodies: A Laboratory Manual, Cold Spring Harbor Laboratory Press, New York, 1999.
[15] D. Armstrong, P.G. Strange, Dopamine D_2 receptor dimer formation: evidence from ligand binding, J. Biol. Chem. 276 (2001) 22621–22629.
[16] J. Sambrook, D.W. Russell, Molecular Cloning: A Laboratory Manual, third ed., Cold Spring Harbor Laboratory Press, New York, 2001. pp. 18.120, 18.122.
[17] T. Kamiya, N. Shioya, O. Saitoh, H. Nakata, Expression of fused receptor for adenosine and dopamine, in: Japanese Biochemical Society 75th Annual Meeting (2002) p. 756.